Available online at www.sciencedirect.com
SCIENCE DIRECT®
Journal of Power Sources 136 (2004) 132–138
JOURNAL OF POWER SOURCES
www.elsevier.com/locate/jpowsour

Electrochemical properties of $LiNi_{0.8}Co_{0.2-x}Al_xO_2$ prepared by a sol–gel method

Chang Joo Han [a], Jang Hyuk Yoon [a], Won Il Cho [b], Ho Jang [a,*]

[a] *Department of Advanced Materials Engineering, College of Engineering, Korea University, 5-1, Anam-dong, Seongbuk-gu, Seoul 136-701, South Korea*

[b] *Eco-Nano Research Center, Korea Institute of Science and Technology, 39-1, Hawolgok-dong, Seongbuk-gu, Seoul 136-791, South Korea*

Received 2 February 2004; accepted 1 May 2004

Available online 3 July 2004

Abstract

Prospective positive-electrode (cathode) materials for a lithium secondary battery, viz., $LiNi_{0.8}Co_{0.2-x}Al_xO_2$ ($x = 0.00$, 0.01, 0.03, and 0.05), were synthesized using a sol–gel method and the structural and electrochemical properties are examined by means of X-ray diffraction, cyclic voltammetry, and charge–discharge tests. The $LiNi_{0.8}Co_{0.2-x}Al_xO_2$ maintains the α-$NaFeO_2$-type layered structure regardless of the aluminium content in the range $x \leq 0.05$. On the other hand, as the aluminium content is increased, the capacity retention of $LiNi_{0.8}Co_{0.2-x}Al_xO_2$ is improved while initial discharge capacity is slightly decreased. Results also show that the current peaks on the cyclic voltammograms are diminished and merged on aluminium addition. This suggests that the improved cycle stability of $LiNi_{0.8}Co_{0.2-x}Al_xO_2$ is due to suppression of the phase transition.

Keywords: Lithium secondary battery; Positive electrode; Sol–gel method; $LiNi_{0.8}Co_{0.2-x}Al_xO_2$; Phase transition

1. Introduction

In recent years, electronic mobile devices have become omnipresent and the rapid progress in various types of mobile devices has led to the fast development and commercialization of secondary batteries. Among them, lithium-ion batteries have been produced on a large scale and used extensively in the commercial mobile devices since they have high working voltage, large capacity, and no memory effect compared with other candidates such as metal-hydride batteries and nickel–cadmium batteries [1]. Increasing demands for longer life and larger capacity have, however, induced further research efforts to improve the electrochemical properties of the lithium-ion battery.

Among the components of lithium-ion batteries, the positive-electrode (cathode) material attracts much attention [2,3]. This is because the composition and structure of the cathode plays a crucial role in effective lithiation and delithiation during the respective charge and discharge processes [4]. Numerous forms of lithium compounds such as $LiCoO_2$ [5], $LiNiO_2$ [6], and $LiMn_2O_4$ [7,8] have been developed for high specific energy and better structural stability. To date, $LiCoO_2$ has been used mainly for cathodes in the commercial lithium batteries due to its superior electrochemical properties. On the other hand, $LiCoO_2$ has high cost, toxicity, and low electrochemical capacity. Thus, $LiNiO_2$ has been developed by replacing Co with Ni for cost reduction, but shows premature fading on long-term cycling and exhibits thermal instability in its charged state since it decomposes at elevated temperatures. $LiMn_2O_4$ also has been studied for lithium-ion batteries because of its low cost, high thermal stability, and non-toxicity. Unfortunately, capacity fading has been reported for $LiMn_2O_4$ due to dissolution of Mn^{2+} from spinel structures into the non-aqueous electrolytes, which causes local structural inhomogeneity and electrolyte decomposition at high voltages.

In order to overcome these shortcomings, $LiNi_{1-x}CO_xO_2$ ($0 < x < 1$) compounds have been developed, based on the fact that $LiCoO_2$ and $LiNiO_2$ have the same layered α-$NaFeO_2$ structure [9–11]. Metals such as Al, Mn, Fe, and

* Corresponding author. Tel.: +82 2 3290 3276; fax: +82 2 928 3584.
E-mail address: hojang@korea.ac.kr (H. Jang).

0378-7753/$ – see front matter © 2004 Elsevier B.V. All rights reserved.
doi:10.1016/j.jpowsour.2004.05.006

Nb also have been used for partial substitution of Ni or Co to enhance the elctrochemical performance of the cathode [12–17]. Among these, Al has attracted much attention since it is known to improve the thermal stability of the lithium nickelate in its charged state by preventing the formation of nickel dioxide and maintaining structural integrity up to 600 °C [18]. It is also known that the intercalation of α-$LiAlO_2$ provides a voltage up to 5 V, which is higher than other lithium transition metal oxides [19]. Therefore, with its non-toxicity and low cost, a solid solution of α-$LiAlO_2$ with lithiated transition metal oxides appears as a viable alternative for a better cathode material.

In this study, structural and electrochemical properties of $LiNi_{0.8}Co_{0.2-x}Al_xO_2$ are investigated by substituting Co with Al in the range of $x \leq 0.05$. The emphasis of the current investigation is to examine the effect of Al doping on capacity retention, cycle stability, and its mechanism.

2. Experimental

Polycrystalline $LiNi_{0.8}Co_{0.2-x}Al_xO_2$ compounds, where $x = 0.00$, 0.01, 0.03, and 0.05, were synthesized by a sol–gel method following the procedure shown in Fig. 1. The gel was formed at 140 °C by mixing $Li(CH_3COO)\cdot 2H_2O$, $(CH_3CO_2)_2Ni\cdot 4H_2O$, $(CH_3CO_2)_2Co\cdot 4H_2O$, and $A1(NO_3)_3\cdot 9H_2O$ with acrylic acid in the distilled water. The gel was fired at 800 °C for 24 h in flowing oxygen to produce the mixture in a polycrystalline form. Composite electrodes were prepared by mixing 84 wt.% of fine $LiNi_{0.8}Co_{0.2-x}Al_xO_2$ particles, 10 wt.% KS6 (conductor), and 6 wt.% polyvinylidene difluoride (PVdF, binder). The mixture was coated on an Al foil and dried at 80 °C for 24 h.

The charge and discharge characteristics of the cathodes were examined in a laboratory pouch cell. The cell comprised a cathode, a lithium metal anode, and a separator. The electrolyte solution was 1 M LiPF6 in a 1:1:1 mixture (by volume) of ethylene carbonate (EC), ethylmethyl carbonate (EMC), and dimethyl carbonate (DMC). Cells were cycled between 4.3 and 3.0 V and the charge and discharge test was carried out at the 1/5*C* rate (0.4 mA cm^{-2}) for the first three cycles, at the 1/3*C* rate for next five cycles, and at the 1/2*C* rate for subsequent cycles. Cyclic voltammograms for bare $LiNi_{0.8}Co_{0.2}O_2$ and Al-doped $LiNi_{0.8}Co_{0.2-x}Al_xO_2$ were obtained in beteween 4.35 and 3.0 at a scan rate of 0.0l mV s^{-1}. The structure and the morphology of $LiNi_{0.8}Co_{0.2-x}M_xO_2$ powders produced by the sol–gel method were investigated by means of scanning electron microscopy (SEM Hitachi S-4300) and X-ray diffraction (RINT/DMAX-2500, RIGAKU).

3. Results and discussion

3.1. Morphology of $LiNi_{0.8}Co_{0.2-x}Al_xO_2$ particles

The size of the $LiNi_{0.8}Co_{0.2-x}Al_xO_2$ particles was examined by SEM since the particle size determines the effective surface area and smaller particles tend to improve the capacity of a battery by reducing the ion diffusion pathway during Li^+ intercalation and deintercalation processes [20]. An electron micrograph of $LiNi_{0.8}Co_{0.2}O_2$ powder prepared by the sol–gel method is presented in Fig. 2. The powder consists of loose fine particles with nanosize adherents on the rounded particle surface. The average size of the particles is less than 1 μm, which is smaller than for those produced

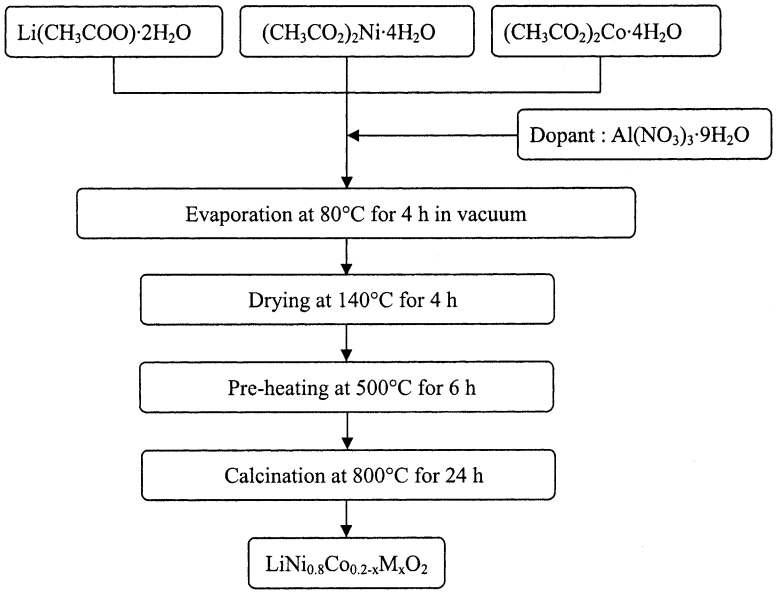

Fig. 1. The experimental procedure for synthesis of $LiNi_{0.8}Co_{0.2-x}Al_xO_2$ powder for $x = 0.00$, 0.01, 0.03, and 0.05 synthesized at 800 °C for 24 h in O_2 atmosphere by sol–gel method.

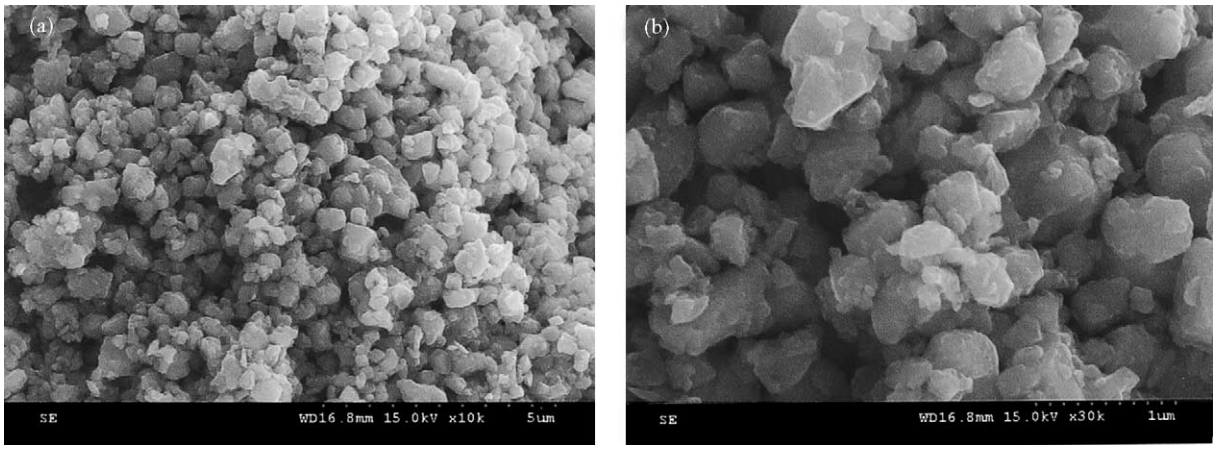

Fig. 2. Electron micrographs of $LiNi_{0.8}Co_{0.2}O_2$ powders synthesized at 800 °C for 24 h in O_2 atmosphere by sol–gel method.

by a solid-state reaction after calcination at the same conditions. The smaller particle size from the sol–gel method is attributed to the small initial particles, which indicates that sol–gel method allows easier size control during calcination treatment.

$LiNi_{0.8}Co_{0.2-x}Al_xO_2$ particles containing different Al contents are shown in Fig. 3(a). A similar size distribution and morphology is observed regardless of the Al content, which indicates that the Al is well permeated into the bare $LiNi_{0.8}Co_{0.2}O_2$ as a solid solution [21]. The successful doping of Al ions into $LiNi_{0.8}Co_{0.2}O_2$ appears to be due to the homogeneous colloidal precursors in the sol before subsequent heat treatments.

3.2. Structure of $LiNi_{0.8}Co_{0.2-x}Al_xO_2$ particles

The crystal structure of $LiNi_{0.8}Co_{0.2-x}Al_xO_2$ particles was investigated by XRD. The resulting diffraction patterns from $LiNi_{0.8}Co_{0.2-x}O_2$ powders prepared by the sol–gel process are given in Fig. 4 and correspond to a layered α-$NaFeO_2$-type structure (space group, *R*-3*m*). They exhibit well-defined (0 0 6)–(1 0 2) and (1 0 8)–(1 1 0) doublets,

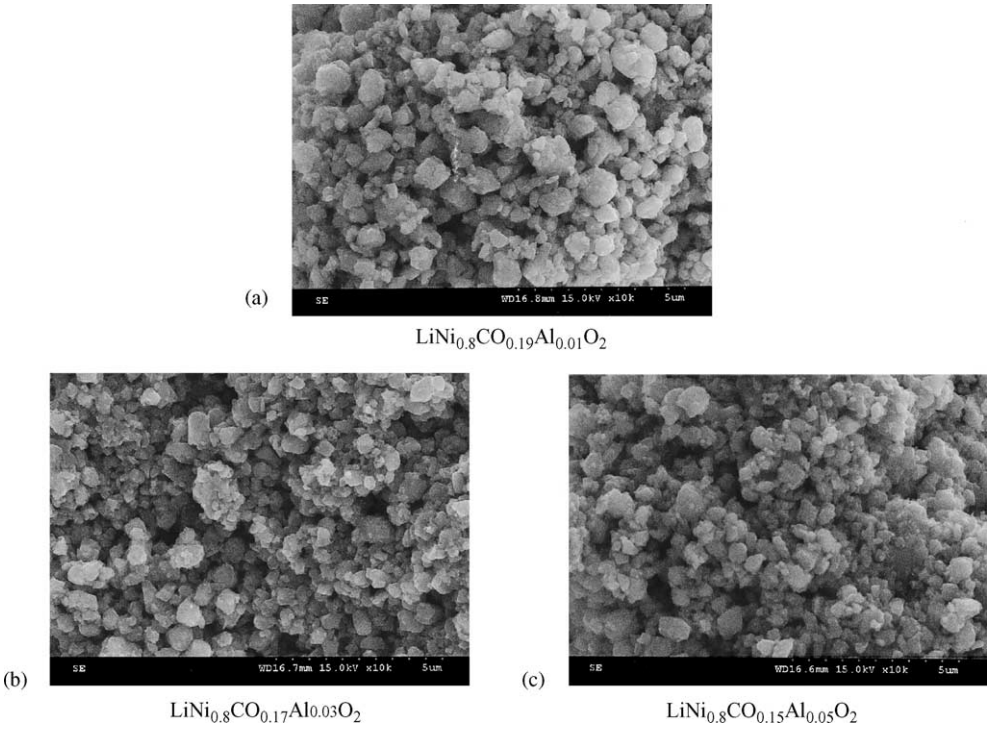

Fig. 3. Electron micrographs of $LiNi_{0.8}Co_{0.2-x}Al_xO_2$ powders for $x = 0.01$ (a), 0.03 (b), and 0.05 (c) synthesized at 800 °C for 24 h in O_2 atmosphere by sol–gel method.

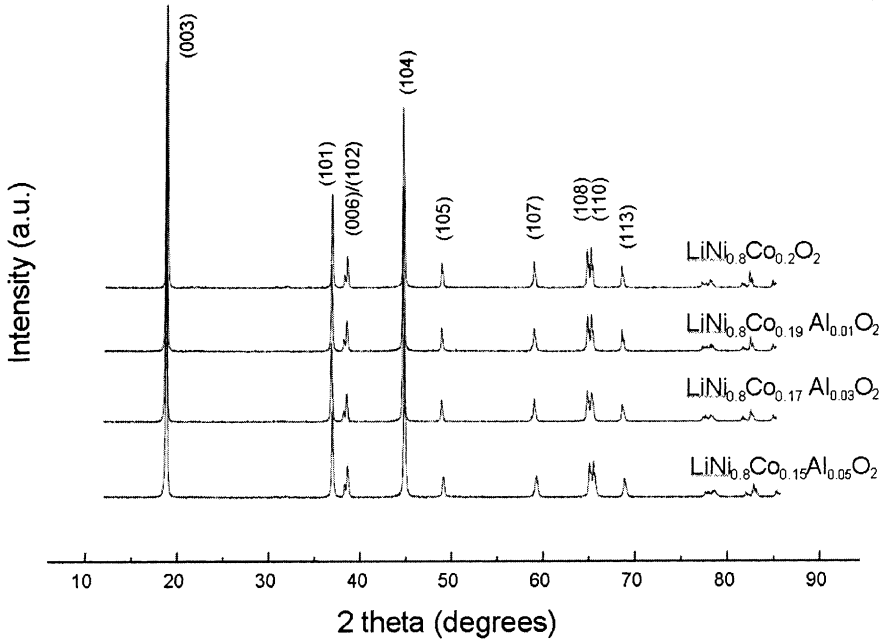

Fig. 4. XRD patterns of $LiNi_{0.8}Co_{0.2-x}Al_xO_2$ powders for $x = 0.00$, 0.01, 0.03, and 0.05 synthesized at 800 °C for 24 h in O_2 atmosphere by sol–gel method.

which indicates an ordered distribution of Li and Ni/Co in a layered structure. These results suggest that $LiNi_{0.8}Co_{0.2}O_2$ forms a solid solution with Al atoms and that the substituted Al atoms are located in the Ni/Co cation sublattices.

The change in lattice parameters as a function of x (Al content) in $LiNi_{0.8}Co_{0.2-x}Al_xO_2$ is presented in Fig. 5. The lattice parameters were obtained, using a least-square method, from experimentally measured XRD profiles. The lattice parameter along the c-axis increases from 14.1539 to 14.1852 Å and a slight change is observed in the a-axis as the Al content increases. The c/a ratio also increases from 4.9418 to 4.9479 due to the substitution of Al ions in the locations of Ni or Co ions and to the ionic character of the Al–O bond [22,23]. The extension of the c-axis represents an increase in the unit-cell volume and facilitates the intercalation and deintercalation of lithium. Thus, the electrochemical properties are improved with increase in Al content.

3.3. Electrochemical properties of $LiNi_{0.8}Co_{0.2-x}Al_xO_2$ particles

Cycle tests were performed at 3.0–4.3 V and 3.0–4.5 V under the same charge–discharge conditions. The cycling performance of the bare $LiNi_{0.8}Co_{0.2}O_2$ and Al-doped $LiNi_{0.8}Co_{0.2-x}Al_xO2$ are shown in Fig. 6. The initial discharge capacity of bare $LiNi_{0.8}Co_{0.2}O_2$ is 181.94 mAh g^{-1} and the initial capacity decreases with Al doping. A minimum capacity of 161.37 mAh g^{-1} is found for $LiNi_{0.8}Co_{0.15}Al_{0.05}O_2$ (Fig. 6(a)). By contrast, the capacity loss of the cathode material is reduced by Al addition. Bare $LiNi_{0.8}Co_{0.2}O_2$ experiences 49% loss in 50 cycles, whereas, only 9% of capacity loss is observed after the same 50 cycle test in the case of $LiNi_{0.8}Co_{0.15}Al_{0.05}O_2$. This trend is more prominent when cycling between 3.0 and 4.5 V, as shown in Fig. 6(b) since it requires greater deintercalation of Li ions from the layered structure. The initial discharge capacity of bare $LiNi_{0.8}Co_{0.2}O_2$ is 223.69 mAh g^{-1} with a drastic capacity loss of 69% in 50 cycles, while the initial discharge capacity of $LiNi0.8Co_{0.15}Al_{0.05}O_2$is 167.85 mAh g^{-1} with 13% capacity loss in 50 cycles. The better capacity retention during cycling tests suggests that Al doping assists maintenance of the original layered crystal structure during deintercalation of Li ions [22,23].

3.4. Cyclic voltammogram of $LiNi_{0.8}Co_{0.2-x}Al_xO_2$ electrodes

Cyclic voltammetry (CV) was used to investigate the electrochemistry of the cathode material $LiNi_{0.8}Co_{0.2-x}Al_xO_2$, as a function of Al content. The shape of the CV curve, peak potentials, and peak currents represent the electrochemical properties of the electrode and disclose the phase transitions that occur during charge–discharge experiments, which strongly affect the capacity fading during cycle [25]. In general, when a cathode experiences phase transformation, a peak occurs in the CV curve due to the coexistence of two phases. During charge–discharge experiments, $LiNiO_2$ shows four different phases (one monoclinic phase, M and three hexagonal phases, H_1, H_2, and H_3) with three peaks in the CV curve [26]. The three peaks in $LiNiO_2$ correspond to

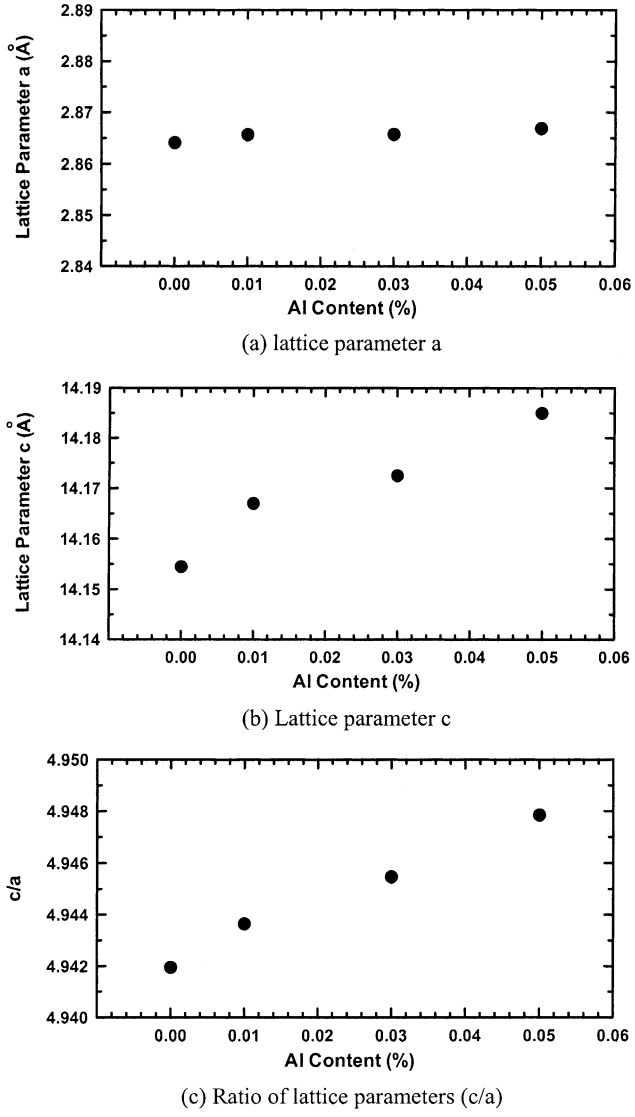

Fig. 5. Lattice parameters of $LiNi_{0.8}Co_{0.2-x}Al_xO_2$ powders for $x = 0.00$, 0.01, 0.03, and 0.05. Lattice parameters *a* (a), *c* (b), and *c*/*a* (c), expressed in hexagonal setting, are plotted as function of Al concentration.

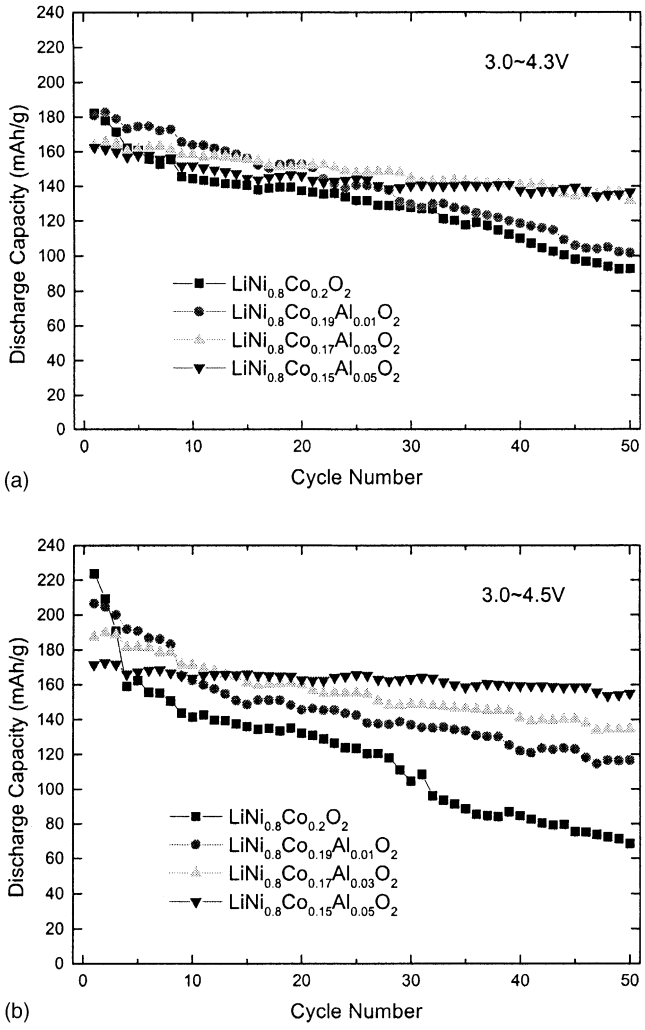

Fig. 6. Plots of discharge capacities of $LiNi_{0.8}Co_{0.2-x}Al_xO_2$ electrode for $x = 0.00$, 0.01, 0.01, and 0.05 as function of cycle number with various charge cut-off voltages. Cycle tests are carried out initially by charging and discharging at 1/5*C* rate for three cycles, followed by five cycles at 1/3*C* rate, and finally at the 1/2*C* rate for a total 50 cycles. Charge and discharge cut-off voltages are between 3.0 and 4.3 V (a) and between 3.0 and 4.5 V (b) at room temperature.

the coexistenc of H_1 and M, M and H_2, and H_2 and H_3, respectively. $LiCoO_2$ also shows four phases (one monoclinic, M and three hexagonal, H_1, H_2, and H_3) in the CV curve [27,28]. The three peaks in $LiCoO_2$ correspond to the coexistence of the phases H_1 and H_2, H_2 and M, and M and H_3.

In this study, cyclic voltammograms of bare $LiNi_{0.8}Co_{0.2}O_2$ and Al-doped $LiNi_{0.8}Co_{0.2-x}Al_xO_2$ are compared in order to deduce the cause of the better capacity retention of $LiNi_{0.8}Co_{0.15}Al_{0.5}O_2$ (Fig. 7). The data clearly show the presence of three peaks at different voltages in $LiNi_{0.8}Co_{0.2}O_2$, which arise from multiple phase transitions during charge–discharge cycling. The second peak in the CV curve for $LiNi_{0.8}Co_{0.2}O_2$, while diminishing in intensity, merges with the first peak with increasing Al content. The first oxidation peak at 3.6 V also shifts to 3.75 V when Al is doped into bare $LiNi_{0.8}Co_{0.2}O_2$. The simplified CV curves and the peak shift are associated with the suppression of phase transitions due to superior maintenance of the layered structure after Al addition. The improved stability of the layered structure is achieved by the presence of electrochemically inactive Al ions in the 3a site, which results better capacity retention during charge–discharge cycling, as shown in the Fig. 6 [24]. This result agrees well with that of Lee et al. [29]. The latter author showed that the structural stability is improved by Co and Al substitution and that fewer phases exist in the cathode during charge–discharge experiments on $LiNi_{0.85}Co_{0.10}M_{0.05}O_2$ (M = Al, Fe).

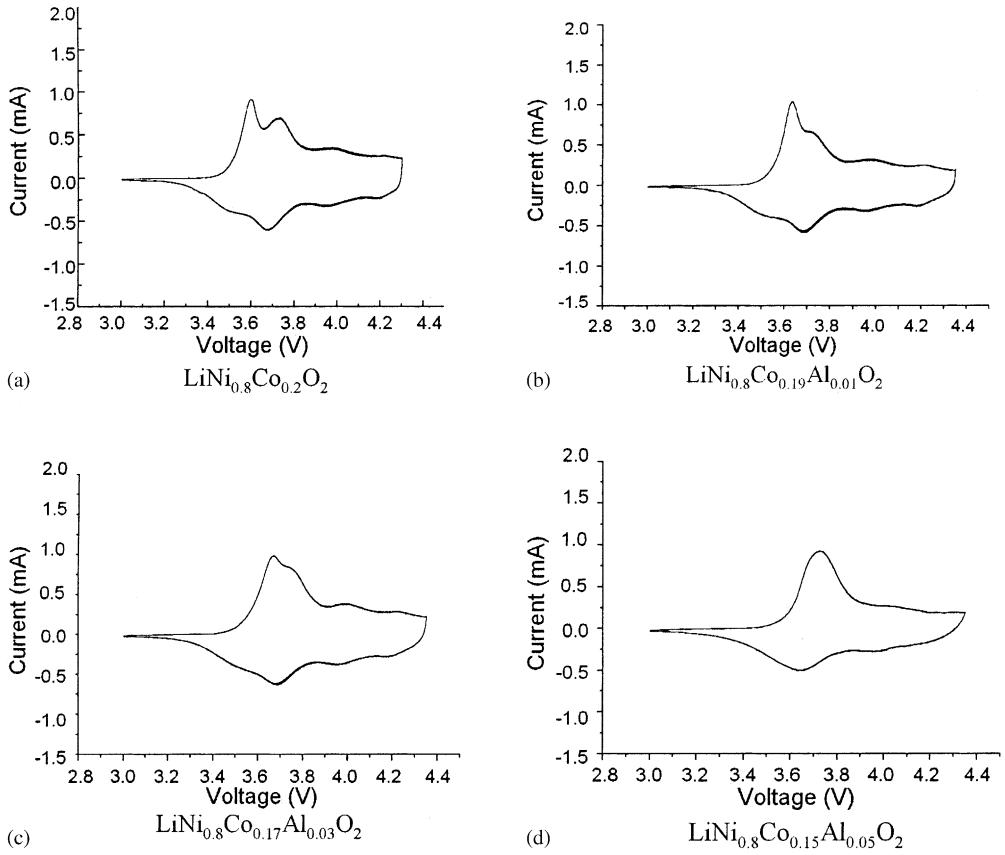

Fig. 7. Cyclic voltamograms $LiNi_{0.8}Co_{0.2-x}Al_xO_2$ powders for $x = 0.00$ (a), 0.01 (b), 0.03 (c), and 0.05 (d). Tests conducted with pouch-type half-cell containing a Li metal anode and a $LiNi_{0.8}Co_{0.2-x}Al_xO_2$ cathode. Voltage scan rate, 0.01 mV s^{-1}.

4. Conclusions

$LiNi_{0.8}Co_{0.2-x}Al_xO_2$ cathodes ($x = 0$, 0.01, 0.03, 0.05), which consist of submicron particles, are fabricated by a sol–gel method. The structural and electrochemical properties are investigated to examined the effect of Al doping on initial discharge capacity and its retention. The cathodes are single-phase compounds regardless of Al content in the range $x \leq 0.05$ and crystallize in a layered structure (space group, *R*-3*m*). The initial discharge capacity decrease as the aluminum content is increased. On the other hand, charge–discharge cycling performance is improved. There is a small capacity loss in the cycle tests between 3.0 and 4.3 V. The relative improvement due to Al doping is more pronounced in the higher voltage range (3.0–4.5 V). The slow degradation of the electrochemical property of Al-doped $LiNi_{0.8}Co_{0.2-x}Al_xO_2$ during cycling is attributed to the suppression of phase transitions by maintaining the layered structure.

Acknowledgements

The research was performed with financial support from the Center for Nanostructure Materials Technology under '21st Century Frontier R&D Programs' of the Ministry of Science and Technology, Korea.

References

[1] K.M. Abaraham, Electrochim. Acta 38 (1993) 1233.
[2] J.R. Dahn, U. von Sacken, M.W. Juzkow, H. Al-Jannaby, J. Electrochem. Soc. 138 (1991) 2207.
[3] C. Delmas, I. Saadoune, Solid State Ionics 53–56 (1992) 370.
[4] H. Wang, Y. Jang, B. Huang, D. Sadoway, Y. Chiang, J. Electrochem. Soc. 146 (1999) 473.
[5] T. Naganuraaftd, K. Tazawa, Prog. Batteries Sol. Cell 9 (1990) 20.
[6] W. Ebner, D. Fouchard, L. Xie, Solid State Ionics 69 (1994) 238.
[7] J.M. Tarascon, E. Wang, F.K. Shokoohi, W.R. Mekinnon, S. Colsons, J. Electrochem. Soc. 38 (1991) 2859.
[8] T. Ohzuku, M. Kitagawa, T. Hirai, J. Electrochem. Soc. 137 (1990) 769.
[9] J. Saadoune, C. Delmas, J. Solid State Chem. 136 (1998) 8.
[10] A.G. Ritchie, C.O. Gowa, J.C. Lee, P. Bowles, A. Gilmour, J. Allen, D.A. Rice, F. Brady, S.C.E. Tsang, J. Power Sources 80 (1999) 98.
[11] D. Caurant, N. Baffler, B. Carcia, J.P. Pereira-Ramos, Solid State Ionics 91 (1996) 45.
[12] T. Ohzuku, A. Ueda, M. Kouguchi, J. Electrochem. Soc. 142 (1995) 4033.
[13] A. Rougier, I. Saadoune, P. Gravereau, P. Willmann, C. Delmas, Solid State Ionics 90 (1996) 83.
[14] H. Arai, S. Okada, Y. Sakurai, J. Yamaki, J. Electrochem. Soc. 144 (1997) 3117.

[15] T. Ohzuku, Y. Makimura, Chem. Lett. 8 (2001) 744.
[16] G. Prado, A. Rougier, L. Fournes, C. Delmas, J. Electrochem. Soc. 147 (2000) 2880.
[17] Y. Sato, T. Kyoano, M. Mukai, K. Kobayakama, Denki Kagaku 66 (1998) 1215.
[18] M.K. Aydinol, A.F. Kohan, G. Ceder, K. Cho, J. Joannopoulos, Phys. Rev. B56 (1997) 1354.
[19] S. Lin, K. Fung, Y.M. Hon, M.-H. Hon, J. Solid State Chem. 167 (2002) 97.
[20] J. Cho, B. Park, J. Power Sources 92 (2001) 35.
[21] S. Castro-Garcia, A. Castro-Couceiro, M.A. Senaris-Rodriguez, F. Soulette, C. Julien, Solid State Ionics 156 (2003) 15.
[22] M. Guilmard, A. Rougier, M. Grune, L. Croguennec, C. Delmas, J. Power Sources 115 (2003) 305.
[23] S. Liu, K. Fung, Y. Hon, M. Hon, J. Solid State Chem. 167 (2002) 97–106.
[24] S. Madhavi, G.V. Subba Rao, B.V.R. Chowdari, S.F.Y. Li, J. Power Sources 93 (2001) 156–162.
[25] K. Dokko, M. Nishizawa, S. Horikoshi, T. Itoh, M. Mohamed, I. Uchida, Electrochem. Solid State Lett. 3 (1999) 3.
[26] W. Li, J.N. Reimer, J.R. Dhan, Solid State Ionics 67 (1993) 123.
[27] J.N. Reimers, J.R. Dhan, J. Electrochem. Soc. 139 (1992) 2091.
[28] T. Ohzuku, A. Ueda, J. Electrochem. Soc. 141 (1994) 2972–2977.
[29] K.K. Lee, W.S. Yoon, K.B. Kim, K.Y. Lee, S.T. Hong, J. Power Sources 97–98 (2001) 308–312.